



Proteome dynamics of the cotyledonary haustorium and endosperm in the course of germination of *Euterpe oleracea* seeds



José R.S. Nascimento^a, Domingos F. Neto^b, Ítalo C. Coutinho^c, Gilberto B. Domont^d, Fábio C.S. Nogueira^{d,e,**}, Francisco A.P. Campos^{a,*}

^a Departamento de Bioquímica e Biologia Molecular, Universidade Federal do Ceará, Fortaleza, CE, Brazil

^b Departamento de Biologia, Universidade Federal do Ceará, Fortaleza, CE, Brazil

^c Departamento de Fitotecnia, Universidade Federal do Ceará, Fortaleza, CE, Brazil

^d Unidade Proteômica, Instituto de Química, Universidade Federal do Rio de Janeiro, Rio de Janeiro, Brazil

^e Laboratório de Proteômica/LADETEC, Instituto de Química, Universidade Federal do Rio de Janeiro, Rio de Janeiro, Brazil

ARTICLE INFO

Keywords:

Euterpe oleracea

Arecaceae

Açaí

Haustrorium

Seed germination

Plant proteomics

Quantitative proteomics

Amazon fruits

ABSTRACT

The role of the cotyledonary haustorium (CH) in the mobilization of nutrient reserves in the endosperm of species of the palm family Arecaceae is a moot question. To shed light on this matter, we present here an analysis of the quantitative proteome changes associated with four developmental stages of CH and three of endosperm during germination. Together, a total of 1965 proteins were identified, being 1538 in the CH and 960 in the endosperm. Both in the CH and endosperm proteomes, we observed an increase in the diversity of hydrolases as the CH and endosperm develops. Qualitative proteomics analysis of four CH developmental stages indicated that each stage is populated by a unique set of proteins and the quantitative analysis showed an increase in the relative abundance of hydrolases, particularly mannan degrading enzymes, as development progresses. These results add weight to the hypothesis that the CH in the seeds of *E. oleracea* acts both as a conduit of carbon and nitrogen sources generated by the hydrolysis of the reserves in the endosperm and as a source of hydrolases that will contribute to the mobilization of these reserves.

1. Introduction

The palm family Arecaceae is one of the largest families of monocotyledons, being restricted to tropical and semi-tropical climates [1]. Many species in this family such as oil palm (*Elaeis guineensis* Jacq), date palm (*Phoenix dactylifera* L.), carnauba palm (*Copernicia prunifera* (Mill.) H.E.Moore), and coconut palm (*Cocos nucifera* L.) are major sources of oil, waxes, edible fruits and nuts [2]. Other species such as the açai palm (*Euterpe oleracea* Mart.), produce fruits which are the source of phytochemicals of great nutritional and pharmacological properties [3,4]. In this family, several issues related to seed germination and seedling establishment are understudied, such as, for instance, the relationship between the cotyledonary haustorium (CH) and endosperm in the mobilization of lipids, carbohydrates, and proteins during germination [5].

The CH is the apical part of the cotyledon that during germination develops into an absorbing structure, being a typical feature of embryos

from the Arecaceae, where they are highly developed [6,7]. The prevailing view about the role of the CH is that it absorbs carbon and nitrogen sources resulting from the digestion of the stored reserves in the endosperm and transferring them to the seedling [8–11]. However, the likelihood that actions of the cotyledonary haustorium are not restricted as a conduit of carbon and nitrogen sources originated by the digestion of endosperm reserves is not discarded. For example, a major unanswered question is whether the cotyledonary haustorium acts as a source of signals that will direct the hydrolysis of reserves within the endosperm [5,12], or whether it acts as the site of synthesis of the hydrolases that upon being transferred to the endosperm, will carry out the mobilization of food reserve [5,9,12–17]. In order to engage in this matter, we have undertaken a quantitative proteome analysis of endosperm and CH obtained from germinating seeds of *E. oleracea* at identical developmental stages. This allowed us to measure the differential abundance of lipases, carbohydrases, and peptidases in these two tissues and ascertain the role of CH as the site of synthesis of hydrolases

* Corresponding authors at: Departamento de Bioquímica e Biologia Molecular, Universidade Federal do Ceará, Campus do Pici, Fortaleza, Ceará, CEP 60451-970, Brazil.

** Corresponding authors at: Laboratório de Proteômica/LADETEC, Instituto de Química, Universidade Federal do Rio de Janeiro, Rio de Janeiro, Brazil.

E-mail addresses: fabiosn@iq.ufrj.br (F.C.S. Nogueira), bioplant@ufc.br (F.A.P. Campos).

<https://doi.org/10.1016/j.plantsci.2020.110569>

Received 12 February 2020; Received in revised form 9 June 2020; Accepted 13 June 2020

Available online 18 June 2020

0168-9452/ © 2020 Elsevier B.V. All rights reserved.

that will be exported to the endosperm to digest the stored reserves.

2. Material and methods

2.1. Plant material

E. oleracea fruits were collected from plants in full fruit production and grown in natural conditions in a commercial cultivation (03° 33' 44" S; 41° 05' 32" W). The seeds were obtained by removing the fruit pericarp and disinfected in 1% sodium hypochlorite for 5 min. Seeds were germinated in autoclaved sand and greenhouse-grown for up to 100 days. Mature seeds and seedlings at 5, 15, 25, 35, 55 days after germination (DAG), were collected, photographed and dissected for the isolation of developing CH and endosperm, except seedlings at 55 DAG, from which only the CH was collected because the endosperm had already been consumed. The seeds were cut open with a sharp blade, and the embryo detached from the endosperm. For the mature seeds and 5 DAG only the tip of the cotyledonary leaf was collected, but for the remaining stages, the globose haustorial portion of the cotyledon was easily discernible and collected. As the seed coat ruminates the endosperm of *E. oleracea*, seeds were sectioned longitudinally, and the sections cut in order to isolate the endosperm from the integument. The collected tissues were washed in cold Milli-Q water and immediately frozen in liquid nitrogen, freeze-dried and stored at -20 °C.

For anatomical analysis, CH from the six analyzed stages were fixed in Karnovsky solution [18], dehydrated in ethanol series of 10–100 % (increased by 10 % per hour) and embedded in histo-resin LEICA for no less than 30 days, sectioned in a rotatory microtome LEICA 2065, stained with 0.5 % toluidine blue in 0.12 % borax combined basic fuchsin 0.5 %.

2.2. Sample processing and protein extraction

The collected material was grouped in three biological replicates, each made up of the relevant tissue from a minimum of 25 seeds. Samples were ground to a fine powder, and protein extraction was carried out according to [19]. 40 mg of samples were added to 800 µL of extraction buffer (500 mM Tris-HCl, 50mMEDTA, 700 mM sucrose, 100 mM KCl, pH 8.0), agitated for 10 min at 4 °C, added of the solution of phenol saturated with 10 mM Tris-HCl, pH 8.0, agitated for 10 min and centrifuged at 5500 g at 4 °C. The phenol phase was collected and a second phenol extraction was done. The phenol phase was precipitated with ice-cold 0.1 M ammonium acetate in methanol at -20 °C overnight. Protein pelleting was carried out by centrifugation at 5500 g 4 °C, and the pellet washed in precipitation solution three times, followed by one wash in cold acetone and dried at room temperature. The pellet was dissolved in 7 M urea/2 M thiourea and protein quantification was obtained using the Bradford assay [20].

2.3. Protein digestion, LC-MS/MS and data analysis

100 µg of protein was subjected to in-solution trypsin digestion as described by [21]. Peptides were solubilized in 0.5 % formic acid, quantified by QuibITM fluorometer (Invitrogen) and the concentration adjusted to 0.5 µg. µL⁻¹. The CH samples were injected in a nano-LC-MS/MS system consisting of an EASY II-nano LC system (Proxeon Biosystem) coupled to a nanoESI LTQ-Orbitrap Velos mass spectrometer (Thermo Fisher Scientific). Two µg of peptides were loaded to a trap column (100 µm × 2 cm) packed in-house with C-18 ReproSil 5 µm resin (Dr. Maisch) and a New Objective PicoFrit analytical column (75 µm × 20 cm) packed with Reprosil-pur C18-AQ 3 µm resin (Dr. Maisch). The gradient applied consisted of phase A (0.1 % formic acid, 5% ACN) and phase B (0.1 % formic acid, 95 % ACN). The gradient started with 5% solvent B and increased to 20 % for 125 min, 20–40 % phase B for 42 min and 95 % phase B for 13 min. Mass spectra were acquired in a positive mode top 10 data-dependent acquisition (DDA) method. MS1

scan was acquired in an Orbitrap analyzer set for a 350–1800 *m/z* range, 30,000 resolution (at *m/z* 400) with a minimal signal required of 5000, isolation width of 2.0. The 10 most intense ions were fragmented by collision-induced dissociation (CID) at 30 normalized collision energy (NCE) with a dynamic exclusion of 30 s. Other mass spectrometric conditions were sheath and auxiliary gas flow 0.0, capillary temperature at 200 °C.

Peptides from endosperm samples were injected in an Easy n-LC 1000 liquid chromatography system (Thermo Scientific, Waltham, MA), with the same trap-column and column system previously mentioned, connected to a Thermo Q Exactive mass spectrometer (Thermo Scientific, Waltham, MA). The gradient used the same solutions mentioned above, starting with a 2% phase B increased to 20 % for 133 min, 20%–40% phase B for 34 min, 40%–95% phase B for 10 min. Mass spectra were obtained in positive mode using a top 15 DDA method. MS1 scan was acquired in the Orbitrap analyzer with a 375–1650 *m/z* interval, 70,000, AGC target of 3e6. The 15 most intense ions were further fragmented in a Higher Energy Collisional Dissociation (HCD) cell at 30 NCE and a dynamic exclusion of 60 s. Other conditions were as follows: spray voltage of 2.76 kV, sheath and auxiliary gas flow of 0.0, capillary temperature of 250 °C. Every biological replicate was run in triplicates so three raw data files were originated. Samples were randomly analyzed. In between samples, a blank injection (0.1 % formic acid) with a 35 min gradient was performed to avoid any residues from the previous sample.

2.4. Data analysis

The raw data files were examined in Xcalibur v.2.1 (Thermo Scientific) and protein identification was carried out by the Proteome Discoverer 2.1 software (Thermo Scientific). The Sequest algorithm was used to obtain the PSM for the analyzed peptides against an Arecaceae family database available at NCBI <https://www.ncbi.nlm.nih.gov/> July 2017 combined with an *Arabidopsis* database downloaded from <http://www.uniprot.org/> July 2017. The parameters used were tryptic cleavage with a maximum of two missed cleavages, methionine oxidation (+ 15,995 Da), carbamidomethylation of cysteine (+ 57,021 Da). The Target Decoy PSM Validator was set to target FDR (strict) 0.01. Only protein identified in a minimum of two replicates were considered for qualitative and quantitative analysis.

2.5. Quantitative analysis

Label-free quantification applying the Precursor Ion Quantifier node from Proteome Discoverer 2.1. were treated by the Perseus 1.6.0.2 software. The quantitative analysis was carried out with the Perseus software downloaded on <http://www.coxdocs.org/doku.php?id=perseus:start/> October 2018. Area values generated by Proteome Discoverer were uploaded, transformed into a logarithmic scale, grouped according to biological replicates, averaged and grouped according to developmental stage, so each stage was represented by three biological replicates, with three technical replicates. CH developmental stages were analyzed by principal component analysis (PCA) in order to evaluate the contrast amongst stages. The filters used were: Filter rows based on valid values, set to consider proteins present in minimal two biological replicates in at least one stage. After data normalization by median subtraction, and statistical evaluation by the ANOVA test, the resulting matrix was filterer for valid values so only protein with statistical significance according to the ANOVA test remained (p-value < 0.05). The resulting area values were subjected to the Post-hoc tests using a FDR of 0.05 and standard deviation between biological replicates.

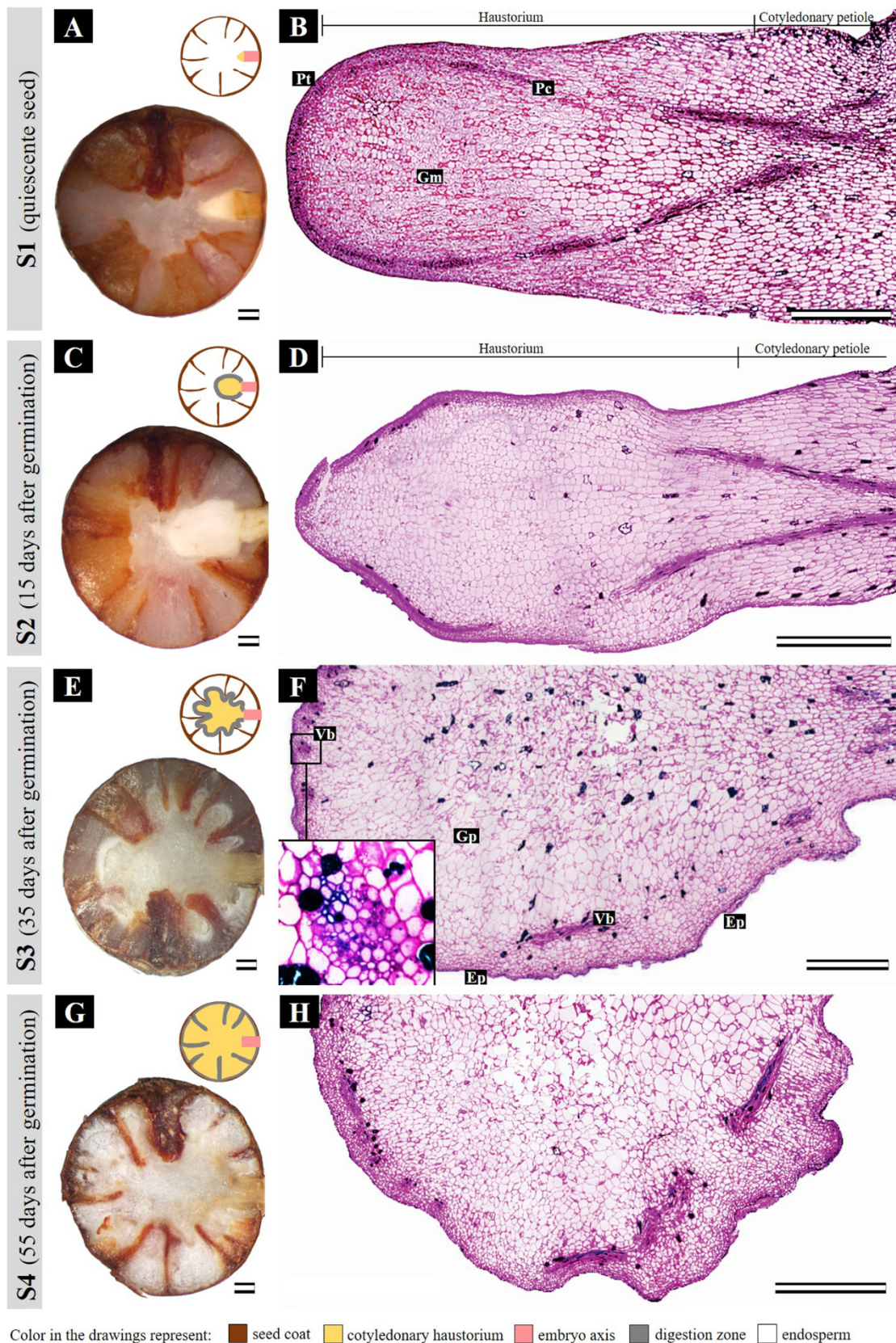


Fig. 1. Development of the cotyledonary haustorium in *E. oleraceae*. (A, C, E and H) Morphological development of the cotyledonary haustorium within the seed with drawings representing each stage. (B, D and F) Longitudinal sections as observed under light microscopy of seed/embryo during the haustorium development. (A, B) S1 stage, the conic haustorium kept within the seed; (C, D) S2 stage, establishment of a digestion zone around the haustorium; (E-F) S3 stage, enlarged haustorium and digestion zone well established at this point. Note the magnification of a collateral vascular bundle in F. (G, H) S4 stage, the haustorium occupying almost the entire seed and little amounts of endosperm are left. Ep, epidermis; Gp, ground parenchyma; Vb, vascular bundle. Scale bar: A, C, E and H = 1 mm; B, D, F, G and I = 500 μm.

3. Results and discussion

3.1. Anatomical development of the cotyledonary haustorium and endosperm from germinating seeds

The developmental stages of germinating seeds were examined by light microscopy. The selection of the stages was based on morpho-anatomical assessments that represent the most distinct stages underwent by the CH and endosperm during their development, vital for the interpretation CH functions in the light of proteome analyses. Four stages (S1, S2, S3 and S4) were selected for the quantitative proteome analysis of the CH and endosperm. At stage 1 (S1), seeds are quiescent, and the brown seed coat incases the ruminant endosperm that occupies most of the seed. Within the seed, two regions are discerned in the conic embryo, the yellowish embryonic axis at the proximal region, and a pale cotyledonary haustorium at the distal region (Fig. 1A, B). Stage 2 (S2), seedlings are at 15 days after the formation of the germinative button. The CH grows into a globular structure mostly due cellular expansions and becomes pressed against the endosperm (Fig. 1C, D). The establishment of a digestion zone also takes place (Fig. 1C, D). At stage 3 (S3), 35 days after formation of the germinative button, the CH development is well underway, the endosperm is partially consumed, and the establishment of a digestion zone placed on the outer side of the haustorium and in contact with the endosperm became evident (Fig. 1E, F). Throughout seedling development, the CH epidermal cells are highly active as they presented large nuclei, often two or three nucleoli, and densely stained cytoplasm. The cytoplasm of epidermal cells is peripheral and displaced towards the outer side, that is, in closer contact with the endosperm. The two or three layers of cells adjacent to the epidermis are bigger than the epidermal cells, but much smaller than the remaining cells of the haustorium. The vascular bundles below the epidermis are more abundant in phloem than xylem and no fibers were observed surrounding it (Fig. 1E, F). The absence of fibers probably facilitates the solute transport into the vascular system. The hard endosperm is mostly composed of cell wall that is consumed at the digestion zone, where the CH is immersed in a gel like interface with the endosperm. At this site, the endosperm cell wall polysaccharides are dismantled by a set of enzymes acting to mobilize seed storage reserves. At S4, 55 days after the formation of the germination button, little or no amounts of endosperm are left, and the CH now occupies almost all the volume within the seed coat (Fig. 1G, H).

3.2. Proteome analysis

Four developmental stages of the cotyledonary haustorium (CH) and three of the endosperm were subjected to proteome analysis (Supplementary Table I). The developmental stage of the endosperm corresponding to S4 of the CH could not be analyzed because this tissue was already mostly consumed (Fig. 1). A total of 1965 proteins were identified with 1538 in the four CH stages and 960 from the three endosperm stages (Table 1). As shown in Supplementary Table I and Fig. 2, CH and endosperm have a divergent set of proteins: A total 1538 proteins were identified from the four CH stages and from these 136 were differently regulated (Supplementary Table II); for endosperm, 960 proteins were identified and from these 49 were differently regulated (Supplementary Table III). The proteome datasets of the developmental stages of the CH were analyzed by principal component

Table 1
Protein identification during the development of the cotyledonary haustorium and endosperm of germination *Euterpe oleracea* seeds.

Developmental stage	S1	S2	S3	S4
Cotyledonary haustorium	500	1146	1065	1051
Endosperm	767	789	551	–

analysis (PCA) (Fig. 3), revealing the uniqueness of the proteome of each dataset, particularly when comparing S1 to later stages. At S1, CH growth has not yet begun and most protein involved in seed reserve mobilization were not detected, indicating that the dynamic changes detected may be causally related to the CH function during germination and seedling establishment.

The CH and endosperm proteomes are populated by a wide variety of proteins related to the dismantling of the cell wall, especially those involved in cell wall reserve mobilizations. Studies with *E. oleracea* and other palms have shown that mannan, a polymer of mannose, is a major component of the cell wall [16] of mature seeds, equivalent to 80 % of the carbohydrates in the seed [22,23] and therefore it comes as no surprise that in this study several species of mannan degrading enzymes such as endo-beta-mannanases were identified from CH and endosperm proteomes (Supplementary table IV). Endo-beta-mannanases (EC:3.2.1.78) were identified for all endosperm developmental stages with an increase in diversity and relative abundance as endosperm consumption progresses (Supplementary table IV and Fig. 4). The identification of mannanases from S1 of endosperm is a strong indicative that these carbohydrases might be stored in the endosperm and activated by some signal originated from the CH during germination, as it has been proposed for *Acrocomia aculeata* [16] and *Butia capitata* [5]. However, some mannanases were identified only for later developmental stages of endosperm, and were also present in the CH (XP_010911540.1, XP_010943133.1) showing the CH as a possible source for these mannan degrading enzymes.

Although mannans are the major reserve for *E. oleracea* seeds, a variety of structural carbohydrates such as glucose, galactose, xylose and arabinose are also present [23]. The diversity of cell wall polysaccharide processing enzymes increases in the same manner of mannanases, being detected for later endosperm stages as well as in the CH. Some of which were up regulated in the endosperm as well as CH (Figs. 4 and 5, Supplementary table II, III and IV). Fig. 1 shows CH development through enlargement of the central cells, so the epidermis and vascular bundles may be pressed against the digestion zone favoring absorption as well as secretion. Accordingly, UDP-glucuronic acid decarboxylase (UXS), responsible for the irreversible conversion of UDP-glucuronic acid into UDP-xylose, the xylose donor for the synthesis of xylan and xyloglucan [24] and UDP-Xyl-4-epimerase (UXE, EC 5.1.3.5) responsible for the conversion of UDP-xylose to UDP-arabinose, used in pectin biosynthesis were identified for CH. Additionally, xylosidases (EC:3.2.1.-, EC:2.4.1.207, EC:3.2.1.177, EC:3.2.1.37) were mostly restricted to the CH. where the set of polygalacturonases, pectinesterases and pectin acetylsterases peaks at S2, when CH growth is at its early stages. The identification of these enzymes to the CH may be casually related to the required cell wall remodeling necessary for CH growth, absorption and secretory role.

Proteins and lipids are also major nutrient reserves in the Arecaceae [25] and accordingly we identified in the endosperm of *E. oleracea* (Supplementary Table IV) a range of seed reserve proteins (e.g. 11S globulin seed storage proteins, 7S globulins, 63 kDa globulin, late embryogenesis abundant proteins, vicilin-like seed storage proteins) some of which decreased in abundance with germination progression (Fig. 6), and a plethora of peptidases which are known to act on the hydrolysis of these reserves during germination (Supplementary Table IV). Also identified in the endosperm proteome was the protein oleosin a major component of lipid droplets known as oil bodies [26], indicating that lipids are an important nutrient reserve in *E. oleracea* endosperm. Additionally, some lipases involved in the fatty acid release from oil bodies were identified to the CH, indicating that the lipid bodies stored in the endosperm are most likely mobilized at the digestion zone. Furthermore, enzymes involved in β -oxidation (thiolase, Acyl-CoA oxidase and Acyl-CoA Synthetase) and glyoxylate cycle (Isocitrate lyase, malate synthase) were identified for both endosperm and CH, indicating that both this tissues are active in lipid catabolism further to fatty acid liberation from oil bodies, especially in CH where

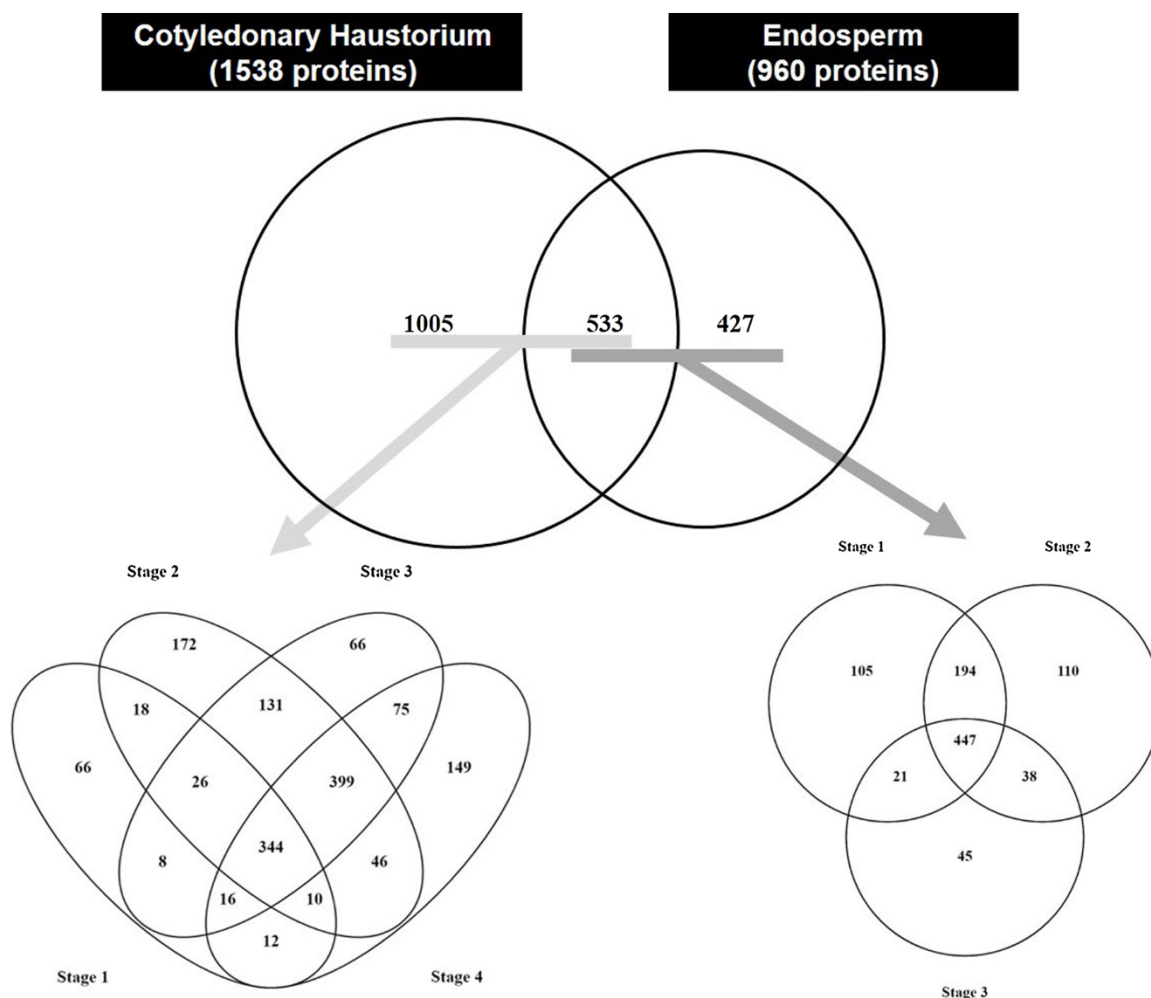


Fig. 2. Venn diagram of proteins identified in developmental stages S1, S2, S3 and S4 from CH and stages S1, S2 and S3 from endosperm of *E. oleracea* germinating seeds.

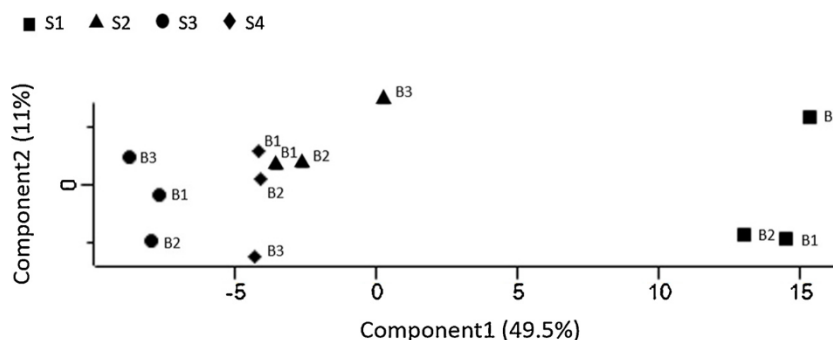


Fig. 3. Principal component analysis (PCA) of proteome datasets of stages S1, S2, S3 and S4 from CH seedling development in *E. oleracea* demonstrating the contrast of proteomes from different developmental stage. Principal components 1 and 2 explain 60.5 % of the variance. B: biological replicate.

malate synthase showed to be up regulated. These data suggests that the oil bodies stored in the endosperm are mobilized by lipases secreted from the CH and the freed fatty acids are catabolized in both endosperm and CH through β -oxidation and glyoxylate cycle, but CH is more active in the glyoxylate cycle, as is well expected to a cotyledonary structure [27]

Table 2 offers a glimpse into the diversity of peptidases, carbohydrases, lipases, and nucleases deposited during the development of the CH and endosperm. The abundance of hydrolases in the CH calls the fact that this structure is apt to digest the endosperm reserves either in the CH itself or, alternatively, by being exported to the CH-endosperm

border. The relative abundance of many of these hydrolases increases as germination progresses (Fig. 5, Supplementary Table III), indicating a likely causal relation with the hydrolysis of the seed reserves within the endosperm. Consonant with the knowledge that carbohydrates, especially mannans, are the major reserve in the endosperm, the largest part of the hydrolases identified in the CH and endosperm are carbohydrases, such as mannan endo-1,4-beta-mannosidase that sharply increases its relative abundance during the first stages of germination (Fig. 4, Supplementary Table II). The relative abundance of certain peptidases, such as a metacaspase involved in programmed cell death is also increased (Supplementary Table III).

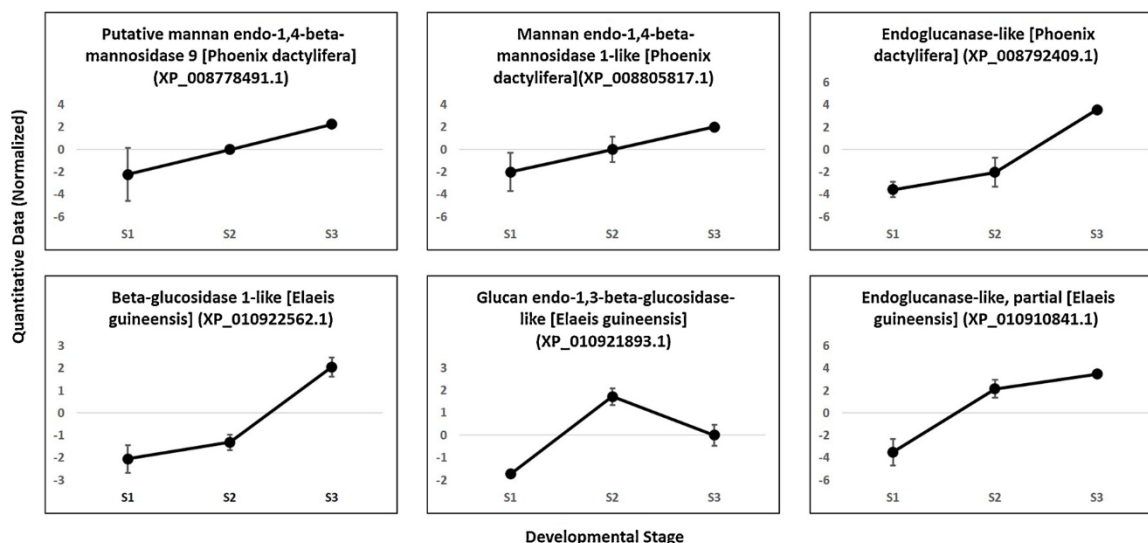


Fig. 4. Quantitative data for proteins involved in cell wall disassembly from endosperm of *E. oleracea* during reserve mobilization. Bars represent the standard deviation of normalized area value for each data point.

We find it significant that we identified in the CH an abundance of proteins related to the redox metabolism, including several peroxidases, catalases, monodehydroascorbate reductase, and superoxide dismutase, and that the relative abundance of many of these proteins, increases as germination progresses (Fig. 4, Supplementary Table II). These enzymes are known to have an important role during seed germination, scavenging reactive oxygen species produced by the intense metabolism associated with the degradation of seed reserves. As with the hydrolases related above, these redox enzymes are likely to be exported to the CH-endosperm boundary to act in concert with the hydrolases responsible for the digestion of the endosperm reserves.

4. Conclusion

A major challenge for the comparative analysis of the endosperm and CH proteomes, lies in the contrasting dynamic range of protein abundance in these tissues, as well as in the limitations of the mass spectrometry methods used. The results presented here reveal the dynamic changes in the proteomes of the CH and endosperm of *Euterpe oleracea* in the course of seed germination. The endosperm proteome is populated by seed storage proteins and by a range of hydrolases, notably carbohydrases, lipases, nucleases and peptidases most of which increase in relative abundance as germination progresses. The CH

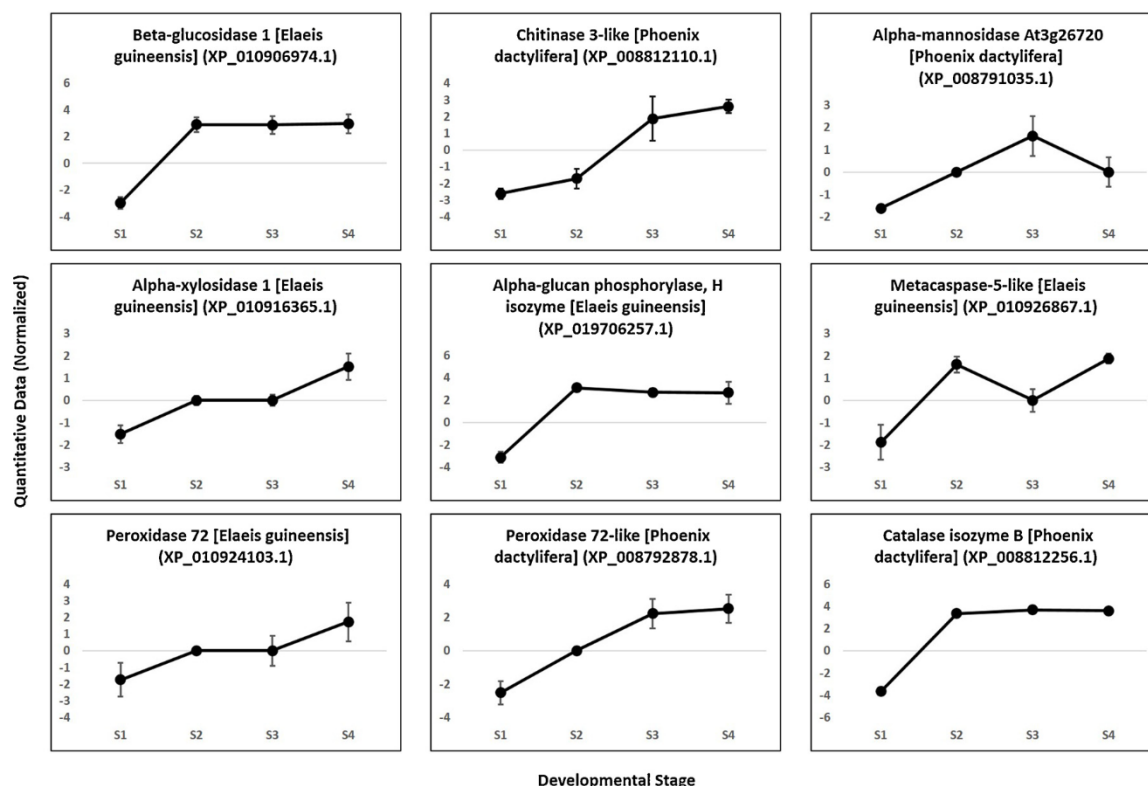


Fig. 5. Quantitative data for hydrolases and proteins related to the redox metabolism during cotyledonary haustorium development in *E. oleracea*. Standard deviation of normalized area value. Bars represent the standard deviation of normalized area value for each data point.

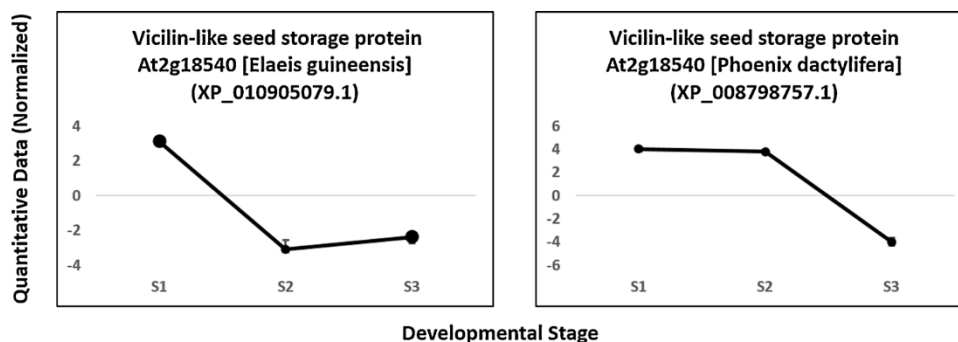


Fig. 6. Quantitative data for storage proteins from endosperm of *E. oleracea* during reserve mobilization. Bars represent the standard deviation of normalized area value for each data point.

Table 2

Identification of hydrolases from cotyledonary haustorium and endosperm of germinating *Euterpe oleracea* seeds.

Tissue	Stage	Peptidases	Carbohydrases	Lipases	Nucleases
Cotyledonary haustorium	S1	15	5	4	0
	S2	37	34	12	1
	S3	41	32	10	2
	S4	39	34	10	1
Endosperm	S1	28	22	4	2
	S2	26	26	2	4
	S3	23	32	3	1

proteome is also populated by hydrolases able to digest seed storage proteins, starch, lipids, nucleic acid and notably the polysaccharides deposited in the cell wall of endosperm cell and which constitute the main nutrient reserve of the seeds. The relative abundance of these enzymes increases as the CH develops leading us to suggest that this tissue is not a mere conduit of carbon and nitrogen sources generated by the hydrolysis of seed reserves in the endosperm, but instead act as a source of hydrolases which are transported to the boundary CH/endosperm.

Declaration of Competing Interest

The authors declare that there is no conflict of interest.

Acknowledgements

This work was financially supported by CNPq (grants 302240/2016-0 to FAPC and 306316/20153 to GBD) and FAPERJ (grant E-26/202.650/2018 to FCSN).

Mass spectrometry raw data and search result files are available at: PRIDE database (Project Name: Proteome Dynamics of the Cotyledonary Haustorium and Endosperm in the Course of Germination of *Euterpe oleracea* Seeds; Project accession: PXD017481).

Reviewer account details: Username: reviewer40538@ebi.ac.uk, Password: J2hYXUbe.

Appendix A. Supplementary data

Supplementary material related to this article can be found, in the online version, at doi:<https://doi.org/10.1016/j.plantsci.2020.110569>.

References

- [1] C. Gomez-Navarro, C. Jaramillo, F. Herrera, S.L. Wing, R. Callejas, Palms (Arecaceae) from a Paleocene rainforest of northern Colombia, *Am. J. Bot.* 96 (2009) 1300–1312, <https://doi.org/10.3732/ajb.0800378>.
- [2] Craig F. Barrett, Christine D. Bacon, A. Alexandre, C. Ángela, H. Tobias, An introduction to plant phylogenomics with a focus on palms, *Bot. J. Linn. Soc.* 182 (2016) 234–255, <https://doi.org/10.1111/boj.12399>.
- [3] D. Pala, P.O. Barbosa, C.T. Silva, M.O. de Souza, F.R. Freitas, A.C.P. Volp, R.C. Maranhão, R.N. de Freitas, Açai (*Euterpe oleracea* Mart.) dietary intake affects plasma lipids, apolipoproteins, cholesterol ester transfer to high-density lipoprotein and redox metabolism: a prospective study in women, *Clin. Nutr.* 37 (2018) 618–623, <https://doi.org/10.1016/j.clnu.2017.02.001>.
- [4] M.T. Andrade, D.F.M. Neto, J.R.S. Nascimento, E.L. Soares, F.A.P. Campos, Proteome Dynamics of the Developing Açaí Berry Pericarp (*Euterpe oleracea* Mart.), (2020), <https://doi.org/10.1021/acs.jproteome.9b00612>.
- [5] D. Souza Dias, L. Monteiro Ribeiro, P. Sérgio Nascimento Lopes, G. Aclécio Melo, M. Müller, S. Munné-Bosch, Haustorium-endosperm relationships and the integration between developmental pathways during reserve mobilization in *Butia capitata* (Arecaceae) seeds, *Ann. Bot.* 122 (2018) 267–277, <https://doi.org/10.1093/aob/mcy065>.
- [6] L.M. Ribeiro, Q.S. Garcia, M. Müller, S. Munné-Bosch, Tissue-specific hormonal profiling during dormancy release in macaw palm seeds, *Physiol. Plant.* 153 (2015) 627–642, <https://doi.org/10.1111/pp1.12269>.
- [7] F. Henderson, A phylogenetic study of Arecaceae based on seedling morphological and anatomical data, *Aliso*. 22 (2017) 251–264, <https://doi.org/10.5642/aliso.20062201.21>.
- [8] F.I. Opute, Lipid composition and the role of the haustorium in the young seedling of the West African oil palm, *Elaeis guineensis* Jacq, *Ann. Bot.* 39 (November (164)) (1975) 1057–1061 Published by: Oxf, 39 (2019) 1057–1061.
- [9] Y. Sugimura, T. Murakami, Structure and function of the haustorium in germinating coconut palm seed, *JARQ, Japan Agric. Res. Q.* 24 (1990) 1–14.
- [10] H.M. Magalhães, P.S.N. Lopes, L.M. Ribeiro, B.F. Sant'Anna-Santos, D.M.T. Oliveira, Structure of the zygotic embryos and seedlings of *Butia capitata* (Arecaceae), *Trees - Struct. Funct.* 27 (2013) 273–283, <https://doi.org/10.1007/s00468-012-0797-1>.
- [11] H.C. Mazzottini-dos-Santos, L.M. Ribeiro, M.O. Mercadante-Simões, B.F. Sant'Anna-Santos, Ontogenesis of the pseudomonomerous fruits of *Acrocomia aculeata* (Arecaceae): a new approach to the development of pyrenarium fruits, *Trees - Struct. Funct.* 29 (2015) 199–214, <https://doi.org/10.1007/s00468-014-1104-0>.
- [12] E.M. Bicalho, T.R.S. dos Santos, Q.S. Garcia, Abscisic acid and the antioxidant system are involved in germination of *butia capitata* seeds, *Acta Bot. Brasiliica* 33 (2019) 174–178, <https://doi.org/10.1590/0102-33062018abb0193>.
- [13] D.A. DeMason, J.I. Stillman, G.S. Ellmore, Acid phosphatase localization in seedling tissues of the palms, *Phoenix dactylifera* and *Washingtonia filifera*, and its relevance to controls of germination, *Can. J. Bot.* 67 (2015) 1103–1110, <https://doi.org/10.1139/b89-144>.
- [14] E.M. Bicalho, S.Y. Motoike, E.E. de Lima e Borges, G. da M. Ataíde, V.M. Guimarães, Enzyme activity and reserve mobilization during Macaw palm (*Acrocomia aculeata*) seed germination, *Acta Bot. Brasiliica* 30 (2016) 438–444, <https://doi.org/10.1590/0102-33062016abb0181>.
- [15] K.N.C. Sekhar, D.A. DeMason, Identification and immunocytochemical localization of α -galactosidase in resting and germinated date palm (*Phoenix dactylifera* L.) seeds, *Planta* 181 (1990) 53–61, <https://doi.org/10.1007/BF00202324>.
- [16] H.C. Mazzottini-dos-Santos, L.M. Ribeiro, D.M.T. Oliveira, Roles of the haustorium and endosperm during the development of seedlings of *Acrocomia aculeata* (Arecaceae): dynamics of reserve mobilization and accumulation, *Protoplasma* 254 (2017) 1563–1578, <https://doi.org/10.1007/s00709-016-1048-x>.
- [17] C. Press, C. Press, *Seedling Development in Washingtonia filifera* (Arecaceae) Author (s): Darleen A. deMason SEEDLING DEVELOPMENT IN WASHINGTONIA FILIFERA, *Mater. Methods Seeds Washingtonia* 149 (2014) 45–56.
- [18] M.J. Karnovsky, A formaldehyde-glutaraldehyde fixative of high osmolality for use in electron microscopy, *Am. Soc. Cell Biol. Source J. Cell Biol.* 27 (1965) 1–149.
- [19] Hervé Thiellement, M. Zivy, C. Damerval, V. Méchin, *Plant Proteomics: Methods and Protocols*, (2007), <https://doi.org/10.1002/9780470988879>.
- [20] M.M. Bradford, A rapid and sensitive method for the quantitation microgram quantities of protein utilizing the principle of protein-dye binding, *Anal. Biochem.* 254 (1976) 248–254.
- [21] M. Shah, E.L. Soares, P.C. Carvalho, A.A. Soares, G.B. Domont, F.C.S. Nogueira, F.A.P. Campos, Proteomic analysis of the endosperm ontogeny of *jatropha curcas* L. seeds, *J. Proteome Res.* 14 (2015) 2557–2568, <https://doi.org/10.1021/acs.jproteome.5b00106>.
- [22] A.F. Monteiro, I.S. Miguez, J.P.R.B. Silva, A.S. Silva, High concentration and yield

- production of mannose from açai (*Euterpe oleracea*) seeds via diluted-acid and mannanase-catalyzed hydrolysis, *Sci. Rep.* (2019) 1–35, <https://doi.org/10.1038/s41598-019-47401-3>.
- [23] M.K.D. Rambo, F.L. Schmidt, M.M.C. Ferreira, Analysis of the lignocellulosic components of biomass residues for biorefinery opportunities, *Talanta* 144 (2015) 696–703, <https://doi.org/10.1016/j.talanta.2015.06.045>.
- [24] B. Kuang, X. Zhao, C. Zhou, W. Zeng, J. Ren, B. Ebert, C.T. Beahan, X. Deng, Q. Zeng, G. Zhou, M.S. Doblin, J.L. Heazlewood, A. Bacic, X. Chen, A.M. Wu, Role of UDP-glucuronic acid decarboxylase in xylan biosynthesis in *Arabidopsis*, *Mol. Plant* 9 (2016) 1119–1131, <https://doi.org/10.1016/j.molp.2016.04.013>.
- [25] U. Patil, S. Benjakul, Characteristics of albumin and globulin from coconut meat and their role in emulsion stability without and with proteolysis, *Food Hydrocoll.* 69 (2017) 220–228, <https://doi.org/10.1016/j.foodhyd.2017.02.006>.
- [26] A. Barre, M. Simplicien, G. Cassan, H. Benoist, P. Rougé, Oil bodies (oleosomes): occurrence, structure, allergenicity, *Rev. Fr. Allergol.* 58 (2018) 574–580, <https://doi.org/10.1016/j.reval.2018.10.005>.
- [27] S. Penfield, S. Graham, I.A. Graham, Storage reserve mobilization in germinating oilseeds: *arabidopsis* as a model system, *Biochem. Soc. Trans.* 33 (2005) 380–383, <https://doi.org/10.1042/BST0330380>.